Neuron, Vol. 24, 127–141, September, 1999, Copyright ©1999 by Cell Press

BMPs as Mediators of Roof Plate Repulsion of Commissural Neurons

Adela Augsburger,† Anita Schuchardt, Sally Hoskins,‡ Jane Dodd,* and Samantha Butler†
Department of Physiology and Cellular Biophysics
Center for Neurobiology and Behavior
Columbia University
New York, New York 10032

Summary

During spinal cord development, commissural (C) neurons, located near the dorsal midline, send axons ventrally and across the floor plate (FP). The trajectory of these axons toward the FP is guided in part by netrins. The mechanisms that guide the early phase of C axon extension, however, have not been resolved. We show that the roof plate (RP) expresses a diffusible activity that repels C axons and orients their growth within the dorsal spinal cord. Bone morphogenetic proteins (BMPs) appear to act as RP-derived chemorepellents that guide the early trajectory of the axons of C neurons in the developing spinal cord: BMP7 mimics the RP repellent activity for C axons in vitro, can act directly to collapse C growth cones, and appears to serve an essential function in RP repulsion of C axons.

Introduction

The projection of axons to their synaptic targets in the developing nervous system is an essential step in the formation of precise neuronal connections. Axon pathway selection depends on environmental guidance cues (Tessier-Lavigne and Goodman, 1996), but, despite the identification of many guidance molecules, understanding how they act together to establish the trajectory of a given class of axons remains a challenge. The embryonic spinal cord represents one region of the vertebrate CNS in which it has been possible to examine the cellular and molecular basis for the complex path of a defined class of neurons. Commissural neurons (C) differentiate in the dorsal spinal cord, adjacent to the roof plate (RP) (Nornes and Das, 1974; Holley, 1982; Altman and Bayer, 1984; Lee et al., 1998), and project to the ventral midline (Ramon y Cajal, 1909; Holley et al., 1982; Wentworth, 1984; Dodd et al., 1988; Oppenheim et al., 1988; Silos-Santiago and Snider, 1992). The axons of newly generated C neurons extend away from the dorsal midline, taking a ventral and circumferential route through the dorsal spinal cord (Figure 1A, 1). In the ventral spinal cord, C axons alter course (Figure 1A, 2), extending medially and ventrally toward the floor plate (FP) (Figure 1A, 3). After crossing the FP, the axons turn orthogonally, join the ventral funiculus, and then project rostrally (Figure 1A, 4) (Holley, 1982; Bovolenta and Dodd, 1990; Yaginuma et al., 1991).

In the ventral spinal cord, netrin-1 (Serafini et al., 1994) and other more locally acting midline cues associated with the FP appear to guide C axons toward and across the ventral midline (Bovolenta and Dodd, 1991; Stoeckli and Landmesser, 1995; Serafini et al., 1996). However, it seems unlikely that these ventral cues also direct the early, circumferential path of C axons. In the absence of an FP, C axons maintain an initial circumferential route that is indistinguishable from their early path in normal embryos (Bovolenta and Dodd, 1991; Placzek et al., 1991). In mice mutant for *netrin-1*, or the netrin-1 receptor subunit *DCC*, the navigation of C axons in dorsal regions appears essentially normal (Serafini et al., 1996; Fazeli et al., 1997).

One source of FP-independent guidance cues for C axons during their initial trajectory may be the RP. The RP is located at the midline of the dorsal spinal cord and, like the FP, acts as a signaling center, playing a major role in the induction and differentiation of neurons in adjacent spinal cord regions (Lee and Jessell, 1999). The inductive capacity of the RP appears to be mediated by members of the TGFβ family of signaling molecules, notably bone morphogenetic proteins (BMPs) (Lee and Jessell, 1999). The RP also expresses ephrins, semaphorins, slits, and glyosaminoglycans (Snow et al., 1990b; Luo et al., 1995; Gale et al., 1996; Wang and Anderson, 1997; Bergemann et al., 1998; Brose et al., 1999; Li et al., 1999), factors implicated in axon guidance in other regions of the CNS. The proximity of C neurons to the RP and the consistency of their initial axonal growth away from the dorsal midline thus raise the possibility that the RP provides guidance cues that repel C axon growth and direct their early trajectory.

We now provide evidence that the RP serves as a local source of a diffusible repellent that orients C axons in vitro. Our results also suggest that BMPs mediate, in large part, the C axon chemorepellent activity of the RP, revealing a novel role for BMPs in the guidance of developing axons in the vertebrate CNS.

Results

The RP Is the Source of a Diffusible Repellent for C Axons

To test the possibility that the initial direction of extension of C axons is regulated by diffusible signals from the RP, we examined whether an explant of the RP repels C axons in vitro. Explants of rat dorsal spinal cord (d-sc explants) were dissected, without RP, from E13, a stage at which many C axons have already extended through the dorsal spinal cord. d-sc explants were grown in a collagen gel, in medium containing netrin-1 to promote the growth of C neurites into the gel (Tessier-Lavigne et al., 1988; Kennedy et al., 1994). RP and control tissue explants (Table 1) were dissected from E11 or E13 rats and placed approximately 100 μm away

*To whom correspondence should be addressed (e-mail: jd18@columbia.edu).
†These authors contributed equally to this work.
‡Present address: Biology Department, City College, City University of New York, New York, New York 10031.

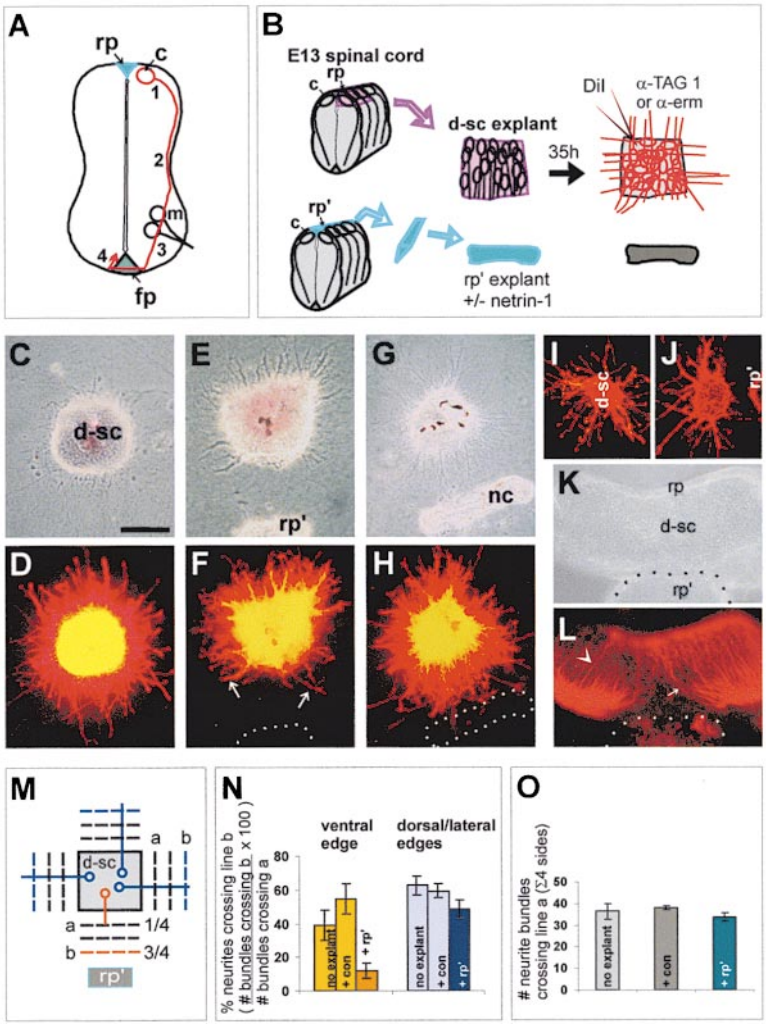

Figure 1. A Diffusible Signal from an RP Explant Reorients C Axons

(A) Transverse section of an E12 rat spinal cord shows trajectory of C axons. Numbers indicate regions of projection described in text.

(B) Experimental design. The d-sc explant comprised the dorsal-most fifth of E13 rat spinal cord (purple), not including adjacent RP. The explant was placed in collagen gel alone or ~100 μm from an E13 RP (rp′) (turquoise) or control tissue explant. Netrin-1 was included to promote C neurite outgrowth. After 35 hr in culture, explants were fixed and labeled with DiI, α-erm, or α-TAG-1. All neurites extending into the gel were TAG-1$^+$.

(C–H) Phase and fluorescence micrographs of d-sc explants labeled with DiI after culture in netrin-1 alone (C and D), with an RP explant (rp′) (E and F), or with E13 rat notochord (nc) (G and H). Arrows in (F) indicate neurites that have apparently veered away from the RP explant.

(I and J) Small d-sc explants, cultured without netrin-1, labeled with α-erm, alone (I), or with an RP explant (rp′) (J).

(K and L) E11 d-sc explant cultured for 35 hr with E11 RP explant (rp′) appended to ventral edge, labeled with α-TAG-1 Ig. Arrow indicates C axons that have altered their direction compared with the straight D–V extension (arrowhead) of axons in regions of the explant not close to the RP explant.

(M) Quantitation of neurite extension. The distance between the d-sc explant and the RP (rp′) or control explant was measured (usually close to 100 μm) and divided by dashed lines. Line a is the line one-quarter of the distance from the edge of the d-sc explant, and line b is the line three-quarters of the distance. In cultures of d-sc explants alone, the total distance was taken to be the same as the average distance between the d-sc explant and rp′s for that experiment. Neurite bundles were traced, and the number crossing lines a and b was counted.

(N) Relative lengths of neurite extension into collagen gel. Orange bars indicate the percentage of neurite bundles that extended as far as line a that also extended as far as line b from ventral edge of d-sc explant cultured alone (38.7 ± 9 SEM, n = 6), with control (54.6 ± 8.7 SEM, n = 11) or with RP explant (12 ± 4.8 SEM, n = 17). Blue bars indicate the percentage of neurite bundles extending from dorsal and lateral edges, not facing RP explant, as far as line a that also extended as far as line b in d-sc explants cultured alone (62.5 ± 5.7 SEM, n = 6), with control (59.3 ± 4 SEM, n = 11) or RP explant (48.7 ± 5.2 SEM, n = 17). (These values show results of experiments with RP explants placed opposite the ventral edge of d-sc explant. Similar results were obtained, independently of side of d-sc explant opposite which RP explant was positioned.) The number of neurites extending from dorsal and lateral edges of d-sc explant with an RP explant was not significantly different from that in d-sc alone ($p = 0.16$) or with a control ($p = 0.12$).

(O) Comparison of total number of neurite bundles (sum of all four sides) extending as far as line a from d-sc explants cultured alone (36.3 ± 3.7 SEM, n = 6), with control (38 ± 1 SEM, n = 11), or RP (33.8 ± 2 SEM, n = 17) explant.

To control for nonspecific effects of the RP on d-sc explant health, acridine orange labeling was used to detect cell death (Graham et al., 1994). There was no evidence of asymmetrical or enhanced levels of cell death in the d-sc explants (n = 10; data not shown). Abbreviations: rp, endogenous RP; rp′, RP explant; c, C neurons; m, motor neurons; fp, floor plate; con, control tissue explant; nc, notochord. Scale bars: (C–H), 100 μm; (I and J), 100 μm; (K and L), 250 μm.

from d-sc explants (Figure 1B). To quantitate neurite outgrowth, we measured the number of neurite bundles extending lengths of one-quarter (line a in Figure 1M) and three-quarters (line b in Figure 1M) of the distance between the d-sc explant and the control or RP explant. In d-sc explants grown alone or with a control explant, bundles of neurites extended into the collagen gel from all sides of the d-sc explant and sometimes contacted the control explant (Figures 1C, 1D, 1G, 1H, and 1N). Of the total number of neurites projecting from the ventral edge of the d-sc explant as far as line a, 47% also reached line b (Figure 1N).

When an RP explant from an E11 or E13 rat spinal cord was placed opposite the ventral edge of the d-sc explant, the length of neurites extending from that edge was reduced by 70%–80% (Figures 1E, 1F, and 1N). Only 12% of neurites projecting to line a extended as far as line b (Figure 1N). Those neurites that did extend further than line a often appeared to have veered away from the RP explant (arrows in Figure 1F). Examination

Table 1. Repellent Activity Is Restricted to Roof Plate and Specific to C Axons

Specificity of Repellent Tissue Source		
E13 d-sc Explant Cultured at a Distance from		**C Axon-Repelling Activity**
E13 RP (spinal cord level)	n = 100	+++
E11 RP (spinal cord level)	n = 30	+++
E13 metanephric mesenchyme	n = 7	±
E13 medial spinal cord	n = 10	−
E13 notochord	n = 6	−
E13 lung epithelium	n = 10	−
E13 ureteric bud	n = 10	−
E13 liver	n = 10	−
E13 heart	n = 10	−
E11 d-sc Explant Cultured with		
E13 RP (spinal cord level)	n = >200	+++
E11 RP (spinal cord level)	n = >200	+++
E13 medial spinal cord	n = 10	−
E13 notochord	n = 10	−
E10 neural plate	n = 10	−
E13 lung	n = 17	−
E13 liver	n = 16	−
E13 heart	n = 15	−
Specificity of Axon Response to the RP		
RP Cultured with		**Axons Repelled**
E13 C axons		+++
E11 C axons		+++
E13 spinal motor axons		−
Retinal axons		−
DRG axons		−

+++, robust repulsion of C axons; ±, small effect on C axons extension; −, no repellent effect

of cultures at 2–5 hr intervals over the 40 hr period in vitro revealed that C neurites did not contact the RP explant (data not shown).

The length and direction of neurites emerging from the dorsal and lateral sides of d-sc explants cultured with an RP explant opposite the ventral edge was not different from that of d-sc explants cultured without an RP explant or with a control explant (Figures 1C–1H and 2B; Table 1). Moreover, the total number of neurite bundles emerging from the d-sc explant as far as line a was not significantly different in control conditions from that in the presence of an RP explant (Figure 1O). These results suggest that there is not a general inhibitory effect of the RP explant on the growth of neurons in the d-sc explants.

Since netrin-1 was used to promote the outgrowth of C neurites, the effect of the RP explant on the extension of C axons could result from the sequestration or inactivation of netrin-1 by factors provided by the RP explant. We therefore tested the effect of RP explants on C axon outgrowth from smaller E13 d-sc explants, which extend C neurites into the collagen gel when grown without netrin-1 (Placzek et al., 1990) (Figure 1I). The pattern of neurite extension from these explants grown alone was approximately radial. In contrast, in the presence of an RP explant positioned at a distance from the d-sc explant, neurite growth on the proximal side was greatly reduced (Figure 1J). Thus, the RP can repel C neurites independently of netrin-1. Taken together, these results provide evidence that the RP secretes a diffusible factor that can repel C axons.

Selectivity of Action of the RP-Derived Repellent

We examined the responses of several other classes of neurons that respond to defined repellents (Luo et al., 1993; Guthrie and Pini, 1995; Loschinger et al., 1997). RP explants were placed in collagen gels at a distance from explants containing spinal motor neurons, dorsal root ganglion (DRG) neurons, or retinal ganglion neurons in conditions that promote their neurite outgrowth. In each case, the direction of neurite outgrowth was unaffected by the presence of an RP explant (Table 1). Thus, only a subpopulation of neurons responds to the repellent activity of the RP.

The RP Signal Can Orient C Axons during their Early Extension in the Spinal Cord

To determine whether RP signals orient C axons within the environment of the dorsal spinal cord, RP explants were placed in contact with d-sc explants taken at E11, a stage at which C axons begin to extend ventrally so that the direction of growth within the explant could be assessed. When explants comprising two to three segments of the dorsal half or two-thirds of E11 spinal cord, including the endogenous RP (see Figure 2A), are cultured for 30–40 hr, in the absence of netrin-1, TAG-1$^+$ axons project through the d-sc explant with a strict dorsal to ventral (D–V) trajectory (Placzek et al., 1990). When a small RP explant was placed touching the cut ventral edge of the d-sc explant (Figure 1K), C axons were deflected from their D–V trajectory (Figure 1L). Initially, axons extended along the D–V axis, but, as they

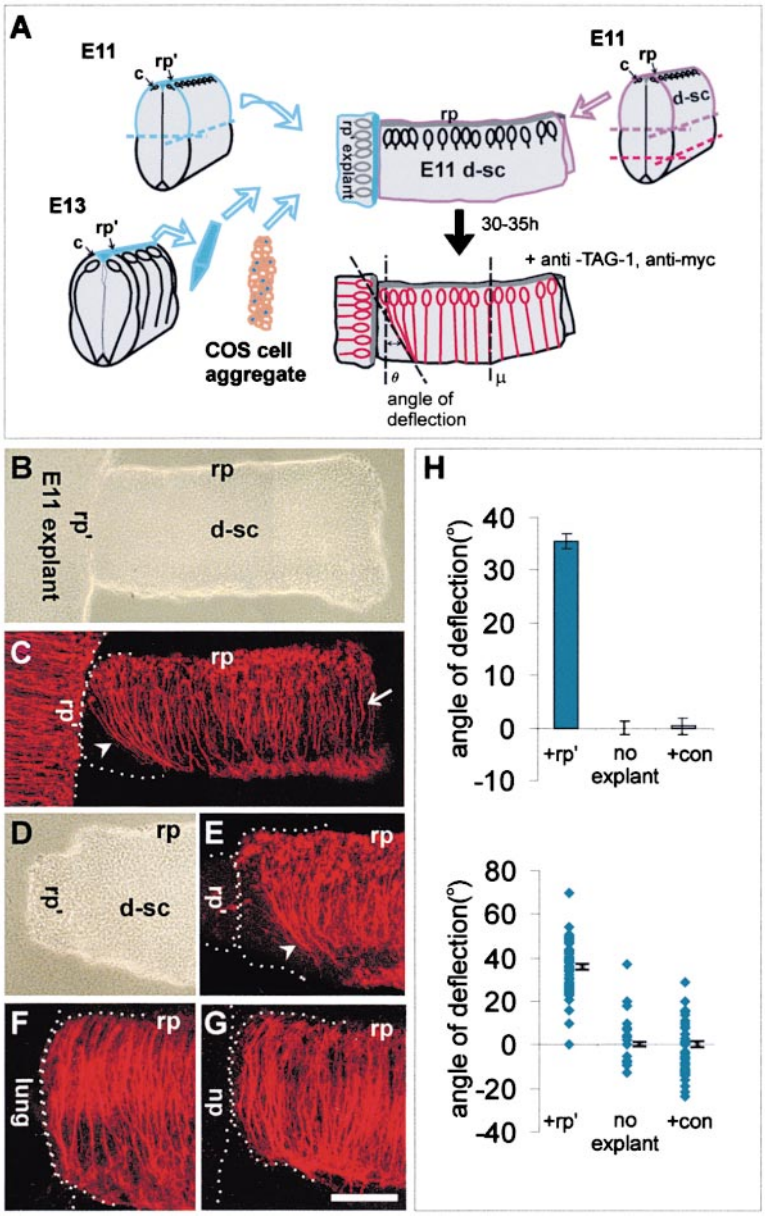

Figure 2. RP Explants Cause Reorientation of C Axons as They First Extend in the Environment of the Dorsal Spinal Cord

(A) Experimental design. A three segment, bilateral piece of E11 dorsal spinal cord (d-sc explant), including the RP (purple outline), often encompassing motor neurons (pink dashed line) was placed in collagen gel with an RP or control explant or COS cell aggregate appended to one end. Ectopic RP explants (rp′) (turquoise) were dissected cleanly at E13, or with adjacent dorsal spinal cord at E11, but placed so that the RP was adjacent to the d-sc explant. Explants were cultured for 30–35 hr, labeled with α-TAG-1 to identify C axons (Dodd et al., 1988) and α-myc (Evan et al., 1985) to monitor COS cell protein, photographed in phase, and imaged by confocal. The direction of extension of C axons was measured as the angle of deflection (θ) from the D–V projection for two or four axons per explant and compared to the D–V projection in other regions of the d-sc explant (μ).

(B–E) Phase and fluorescence (collapsed Z series confocal images of explants in this and all subsequent figures) micrographs of TAG-1-labeled d-sc explant with E11 RP (rp′) (B and C) or an E13 RP explant (D and E) appended. C axons extend directly D–V at the control end of the d-sc explant (arrow). Near the appended RP explant, C axons in the d-sc explant are deflected (arrowheads in [C] and [E]). To assess the possibility that C axon reorientation from the appended RP was caused nonspecifically by contact between the explants, we also examined the direction of C axons when an RP explant was placed at a distance from the edge of the d-sc explant. C axons reoriented (data not shown).

(F and G) TAG-1-labeled d-sc explants with appended control explants of E13 lung (F) and E10 caudal neural plate (G).

(H) Histograms show the average (top) and the range, mean, and SEM (bottom) of angles of deflection of C axons in d-sc explants with ectopic RP, alone, or with control tissue explants. The average deflection of C axons by RP explants was 35.4° ± 1.4 SEM, n = 60. In contrast, the average angles in the absence of an appended explant or with a control explant were 0.02° ± 1.2 SEM, n = 70, and 0.4 ± 1.5 SEM, n = 58, respectively.

Scale bars: (B and C), 250 μm; (D and E), 225 μm.

came within approximately 150 μm of the RP explant, they altered the direction of growth, to veer away from the explant. Axons in other regions of the d-sc explant maintained a normal D–V trajectory (arrowhead in Figure 1L). Thus, the RP explant can orient C axons within the neural epithelium.

We next examined whether C axons respond to the RP signal at the time they navigate away from the midline within dorsal spinal cord. An RP explant was appended to one end of the E11 d-sc explant (Figure 2A) adjacent to C axons at that end as they first extend. Axons in regions of the d-sc explant far from the appended RP projected along a D–V trajectory (as in line μ in Figure 2A; arrow in Figure 2C; Figure 2H). In contrast, C axons extending within 100–150 μm of the appended RP explant were deflected from their D–V trajectory (arrowheads in Figures 2C and 2E) by an average angle of 35° away from the edge to which the RP explant was appended (Figure 2H). E13 notochord (Figures 1G, 1H, and 1N), E10 caudal neural plate (Figure 2G), and E13 heart, lung (Figure 2F), and liver were ineffective in reorienting C neurite growth (Table 1). E13 metanephric mesenchyme did express repellent activity at a low level (Table 1).

We also examined whether chemorepellent activity is differentially distributed in the spinal cord. Explants of E11 or E13 intermediate spinal cord, the region through which C axons project after their initial ventral growth away from the RP, did not affect the direction of C axon extension (Table 1). Thus, within dorsal spinal cord, repellent activity appears to be localized to cells in and around the RP.

Reorientation of C Axons Is Independent of RP Inductive Activity

Signals from the RP induce dorsal spinal cord cell types (Lee and Jessell, 1999). We therefore considered whether the reorientation of C axons within d-sc explants by the RP could be secondary to a local change in cell differentiation within the dorsal neural epithelium.

We determined, first, whether the response of C axons to the RP signal occurs with a time course briefer than that required for induction of dorsal cells in explants (~24 hr; Liem et al., 1997). By 15 hr, the earliest time at which orientation could be assessed, C axons had reoriented away from the RP explant (data not shown). This argues against the idea that the induction of dorsal cell types and subsequent formation of an axon scaffold or secondary signaling center accounts for the observed repulsion of C axons.

We then tested directly whether three dorsal spinal cord cell types induced by RP differentiated in the d-sc explant in response to the RP explant. Antibodies against markers of the RP (MafB; Lee et al., 1998; Figure 3A), of D1 neurons and their precursors (LH2; Liem et al., 1997; Figure 3G) (mATH-1; Helms and Johnson, 1998; Figure 3D), and of D2 neurons (Isl-1; Liem et al., 1997; Figure 3J) were used to identify dorsal cell types. C axons were reoriented in the region of the d-sc explant adjacent to the RP explant, but neither RP nor D1 or D2 neuron markers were ectopically induced (Figure 3). Thus, the reorientation of C axons by the RP explant is not a secondary consequence of the induction of known dorsal cell types.

BMPs Mimic the RP Chemorepellent Activity

The RP expresses semaphorins and ephrins as well as wnts and certain cell surface molecules that might act as repellent signals. Several of these factors were tested but failed to mimic RP activity (data not shown; Table 2). We next considered the possibility that BMPs mediate the repellent activity of the RP.

First, we examined which *Bmp*s are expressed by the rat RP at spinal cord levels. *Bmp6* and *Bmp7*, members of the *BMP5–7* subgroup (Celeste et al., 1990; Hahn et al., 1992; Gitelman et al., 1997), and *Gdf7*, a member of a distinct subgroup of *BMP*s (Lee et al., 1998), are expressed in the rat RP at the time during which C axon extension occurs (E11–E13) (Figure 4). *Bmp7* expression in the RP appeared restricted to a midline subset of the cells expressing *Bmp6* and *Gdf7* (Figures 4B and 4D). In addition, *Bmp7* expression was observed at lower levels in a bilateral patch of cells in the dorsal ventricular zone (arrow in Figure 4B), just ventral to the RP and medial to the position of differentiating C neurons. *Bmp5*, the third member of the *BMP5–7* subclass, and *Bmp4*, a member of the *BMP2/4* subgroup, were not detected. The profile of *Bmp* expression by rat RP thus appears to be identical to that in mouse RP (Jones et al. 1991; Lyons et al., 1995; Dudley and Robertson, 1997; Furuta et al., 1997; Lee et al., 1998).

To determine whether BMPs can mimic the activity of the RP in orienting C axons, chick and mouse cDNAs encoding Bmps, tagged with a myc epitope sequence were expressed in COS cells, and aggregates of *Bmp*- or vector-transfected COS cells were placed at one end of d-sc explants (Figure 2A).

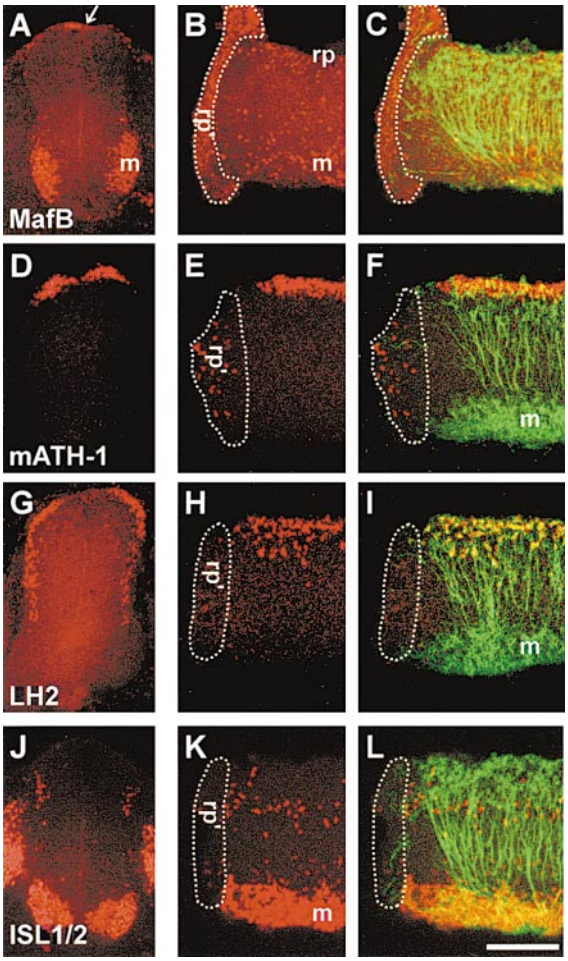

Figure 3. RP Explants Do Not Induce Ectopic Dorsal Cell Markers in the E11 d-sc Explants

(A, D, G, and J) Transverse sections of E12 rat spinal cord labeled with antibodies show the normal distribution of dorsal cell markers. (B–L) d-sc explants cultured with E13 RP explants (rp′) for 25 hr, double-labeled with antibodies against dorsal markers (red) and α-TAG-1 (green). (B, E, H, and K) Marker expression alone. (C, F, I, and L) Double label of markers and C axons. Although deflection of C axons consistently occurred, ectopic expression of the dorsal cell markers was not observed.

(A–C) MafB is expressed in the RP (arrow) and also in the ventral two-thirds of the spinal cord, in motor neurons (m) and ventral interneurons. In E11 d-sc explants after culture, RP labeling is lost, but normal MafB expression is observed in interneurons and motor neurons.

(D–F) mATH-1 is expressed in dorsal interneuron progenitor cells, adjacent to the RP. MATH-1$^+$ cells were also found in the d-sc explants and sometimes in the appended RP explant.

(G–I) LH2A/LH2B$^+$ dorsal sensory neurons, including C neurons, flank the RP and migrate ventrolaterally. Expression was unchanged in the d-sc explants.

(J–L) Isl1 is expressed in a subpopulation of dorsal sensory neurons (arrowhead) and in motor neurons (m) in E12 spinal cord. Normal expression was found in d-sc explants with an appended RP.

Abbreviations: rp, endogenous RP; rp′, ectopic RP explant; m, motor neurons. Scale bars: (A, D, G, and J), 250 μm; (B, C, E, F, H, I, K, and L), 220 μm.

When exposed to COS cells expressing BMP7, C axons within approximately 150 μm were reoriented away from the source of BMP (Figures 5A–5C). The angle of deflection from the D–V axis was 31° (Figure 5M), a value

Table 2. BMPs Mimic RP Activity

Factors Tested for Their Ability to Reorient C Axons		C Axon-Repelling Activity
Potential C Axon Guidance Factors Expressed by the RP and Family Members Tested		
E13 d-sc explant		
Collapsin 2	(Luo et al., 1995)	−
SemaIII/collapsin 1	(Luo et al., 1993)	−
Ephrins	(Gale et al., 1996)	−
E11 d-sc explant		
Wnt1	(Parr et al., 1993)	−
Wnt3	(Roelink and Nusse, 1991) (Parr et al., 1993)	−
Wnt3a	(Roelink and Nusse, 1991) (Parr et al., 1993)	−
Wnt4	(Parr et al., 1993)	−
TGFβ Family Members		
E11 d-sc explant		
BMP7	(see Lee et al., 1998)	+++
BMP6	(see Lee et al., 1998)	±
GDF7	(Lee et al., 1998)	−
BMP4	(Jones et al., 1991)	+++
ActβB	(Liem et al., 1997)	−
DS11	(Basler et al., 1993)	−
CVg1	(Shah et al., 1997)	−

Collapsins, wnts, and BMPs were tested by expression in COS cells as described in the text. All constructs were tagged with myc to demonstrate protein expression. Collapsins were examined for their ability to repel C axons in collagen gel. The potential involvement of ephrins was tested using blocking reagents provided by N. Gale and G. Yancopoulos (Regeneron). Neither Elk Ig nor Ehk Ig altered the ability of the RP explant to repel C axons. Wnts were examined for their ability to reorient C axons in E11 neuroepithelium. C axons frequently grew into aggregates of COS cells expressing wnts.
+++, robust repulsion of C axons with angle of deflection $> 30°$; ±, small but significant repulsion with angle of deflection $= 7°$; −, no deflection.

similar to that evoked by an RP explant (Figure 2M). Vector-transfected COS cells did not repel C axons (Figures 5D–5F and 5M, average deflection of $-1°$). BMP6, another member of the BMP5–7 subclass expressed in the RP, had a much smaller effect on the direction of C axon extension (Figures 5G–5I and 5M), eliciting a deflection of 7°. COS cells expressing GDF7 did not significantly alter the C axon trajectory (Figures 5J–5L and 5M).

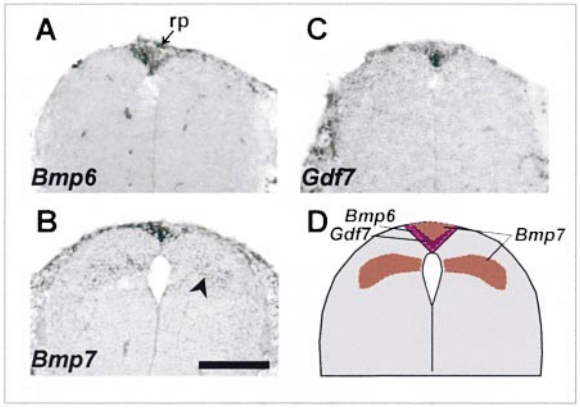

Figure 4. *Bmp* Expression in the RP of the E11 Rat Spinal Cord

(A–C) *Bmp6*, *Bmp7*, and *Gdf7* are all expressed at the dorsal midline, in the RP (rp). (D) shows the relative sizes of domains of expression in the RP. In addition, *Bmp7* is expressed at a lower level bilaterally in the dorsal venticular zone (arrowhead in [B]). Scale bar, 90 μm.

To examine further the specificity of the response of C axons to BMPs, we tested other BMPs and members of the TGFβ superfamily. *Bmp4* is expressed in the dorsal midline of the forebrain of the mouse and in the spinal RP of chick, *Dsl1* is expressed in the dorsal midline of the chick spinal cord, and *ActβB* and *Vg1* in broader dorsal domains (Jones et al., 1991; Basler et al., 1993; Furuta et al., 1997; Liem et al., 1997; Shah et al., 1997). Of these, only BMP4 reoriented C axons, causing a deflection similar to that evoked by BMP7 (average angle ≈ 30°, n = 8; data not shown) (Table 2).

Reorientation of C Axons by BMP7 Is Distinct from Its Ability to Induce RP or Dorsal Neurons

BMPs expressed by rodent and chick RP cells mediate the ability of the RP to induce both RP cells and dorsal sensory relay neurons (Lee and Jessel, 1999). Even though RP explants did not induce ectopic dorsal cells in the d-sc explant (Figure 3), BMPs may be delivered at much higher concentrations from COS cells than from the RP. The ability of BMP7 and BMP6 to reorient C axons might therefore be secondary to a change in the identity of cells in the d-sc explant. However, members of the TGFβ family, including GDF7, Dsl1, and ActβB, are as effective as BMP7, BMP6, and BMP4 in inducing dorsal neural cells in chick and mouse yet do not mimic the orienting activity of the RP (Figure 5; Table 2). This raises the possibility that the axon reorienting and inductive activities of BMPs are distinct but does not address directly whether the orienting response to BMP7 depends on its inductive activity. We therefore examined

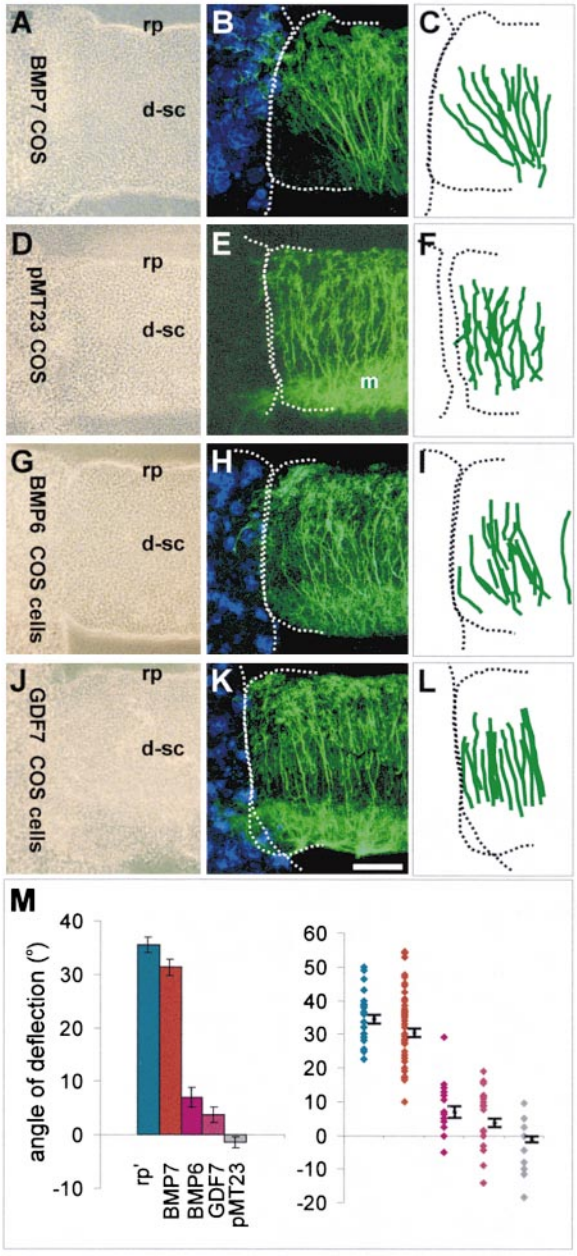

Figure 5. BMP7 Mimics the Repellent Action of the RP

(A–L) Phase and fluorescence micrographs and computer tracings of axons of a TAG-1-labeled (green) d-sc explant with COS cells (labeled with α-myc [blue] when expressing BMPs) appended. Motor neurons ([m] in [E]) were present in some of these d-sc explants but were in normal positions throughout the explant, and their presence or absence in our experiments did not affect the results.

(A–C) COS cells expressing BMP7 caused a deflection of C axons similar to that evoked by RP (Figure 2). The other ends (distal to COS cell pellet) of all explants shown in this and other figures had normal D–V axon projections.

(D–F) Vector-transfected COS cells (not labeled with α-myc) do not evoke the deflection of C axons. In both BMP- and vector-transfected conditions, TAG-1$^+$ neurites occasionally extend into the COS cell pellet (see also Kennedy et al., 1994).

(G–L) BMP6 was weakly active in deflecting C axons (H and I), whereas GDF7 appeared not to repel C axons (K and L).

(M) Histograms of angles (left) and range, mean, and SEM (right) of angles of axon deflection evoked by RP explants (rp′, aquamarine bar) or COS cells transfected with *BMP*s (brown and purple bars) or with pMT23 alone (grey bar). RP explants caused an average deflection of 35.4° ± 1.4 SEM (n = 60). BMP7 caused a deflection of 31.3° ± 1.5 (n = 49). BMP6 evoked a deflection of 7.0° ± 2.2 SEM (n = 18). This is significantly (t test, $p < 0.001$) different from the control angle evoked by pMT23-transfected COS cells (1.4° ± 1.0 SEM (n = 27). GDF7, however, caused a deflection of 3.7° ± 1.5 SEM (n = 28) that was not significantly different from controls. Scale bar, 100 μm.

whether the reorientation of C axons and the induction of dorsal cells by BMP7 are elicited at different concentration thresholds, permitting the two activities to be dissociated.

BMP7-expressing COS cells were mixed in different ratios with vector-transfected COS cells such that aggregates contained 0%, 10%, 25%, 50%, or 100% *BMP7*-transfected cells (BMP7-COS cells). The direction of C axon extension and the expression of MafB or mATH-1 were monitored in d-sc explants that had been cultured with COS cell aggregates for 30 hr (Figure 6). The threshold for deflection of C axons was reached when the aggregate contained 10% BMP7-COS cells (Figures 6E and 6F) and was robust at 25% (Figures 6H and 6I). In contrast, ectopic induction of MafB (Figure 6J) or mATH-1 (Figures 6O and 6P) was consistently observed only with 100% BMP7-COS cells. Thus, reorientation of C axons was observed at a concentration of BMP7 approximately 4- to 10-fold lower than that required for the induction of dorsal cell types, providing evidence that the ability of BMP7 to reorient axons is distinct from its ability to induce RP cells.

We next examined whether the apparent specificity of the axonal response to different BMPs results instead from marked differences in the levels of BMPs secreted by the COS cells. COS cells expressing BMP7, BMP6, and GDF7 each induced mATH-1 (Figures 6O–6R and data not shown) and MafB (Figures 6J–6L, 6S, and 6T and data not shown) to similar levels but did not induce LH2 or Isl1 (data not shown). Robust reorientation of C axons was observed only in response to BMP7 (Figures 6H, 6K, 6N, 6P, and 6T). Thus, reorientation of C axons by BMPs does not appear to be a secondary consequence of the induction of intermediary dorsal cell types. Furthermore, these results raise the possibility that the structure–function relationships of BMPs in dorsal cell induction and axon orientation assays differ.

Antagonism of BMP Action Blocks the Repellent Activity of the RP

To test the involvement of BMPs as endogenous axon guidance molecules provided by the RP, we used three methods of attenuating BMP activity: soluble inhibitors of BMP action, anti-BMP antibodies, and genetic elimination of *Bmp7*.

Follistatin Blocks the RP Repellent Activity

To examine the dependence of the RP activity on BMPs, follistatin, an inhibitor of the BMP5–7 subclass, or noggin, an antagonist of the BMP2/4 subclass and GDF7 (Yamashita et al., 1995; Zimmerman et al., 1996; Liem et al., 1997; Lee et al., 1998), was added to d-sc explants cultured with RP. Whereas C axons reorient with an

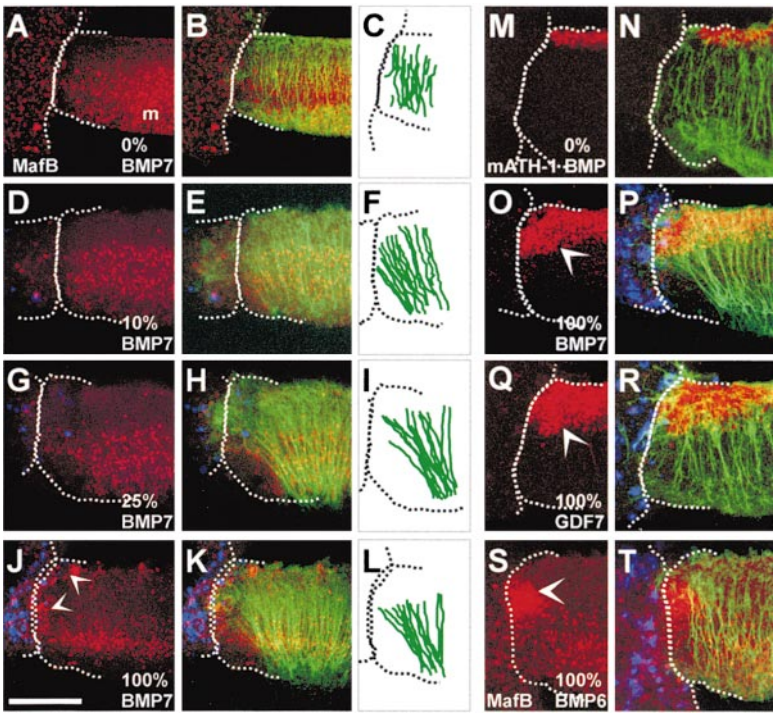

Figure 6. Reorientation of C Axons in Dorsal Explants Is Independent of Inductive Ability of BMPs

(A–L) Dose–response curve for the effect of BMP7 on MafB expression (red) and C axon (green) deflection. (A, D, G, and J) Distribution of MafB. (B, E, H, and K) Triple-labeled explants with α-TAG1 (green), α-myc (blue), and α-MafB (red).

(A–C) COS cell aggregates containing cells expressing vector alone did not induce ectopic MafB or deflect axons in the d-sc explant.

(D–L) C axon deflection was first observed when BMP7-COS cells represented 10% of the aggregate (D–F) and was robust at 25% (G–I). Ectopic induction of MafB (arrowheads in [J]) occurred consistently only when BMP7-transfected cells represented 100% of the aggregate (J–L).

(J–T) BMP7, BMP6, and GDF7 all induce mATH-1 (M–R) and MafB (J, K, S, and T) in d-sc explants.

(M and N) d-sc explant cultured with COS cells expressing vector alone to illustrate the control distribution of mATH-1 (red) in a d-sc explant.

(O–T) COS cell aggregates with *BMP7*-, *GDF7*-, or *BMP6*-transfected cells only.

(O and P) Ectopic mATH-1 was expressed (arrowhead in [O]), and C axons were deflected (P).

(Q and R) GDF7 also induced ectopic mATH-1 (arrowhead in [Q]) but did not cause C axon deflection (R).

(S and T) BMP6 induced ectopic MafB (arrowhead in [S]; compare with induction in [J]), but axons were not deflected (T). The inability of the BMPs to induce either LH2 or Isl1 (data not shown) despite the induction of RP and dorsal cell precursors may reflect the reduced competence of the d-sc due to the developmental stage of E11 rat spinal cord.

Scale bar, 200 μm.

average angle of deflection of 35° in d-sc explants incubated with a RP alone, in the presence of follistatin the angle was reduced to 19° (Figures 7C, 7D, and 7G). In contrast, noggin did not block the repellent activity of the RP (data not shown). In explants cultured with both follistatin and noggin, the repellent action of the RP

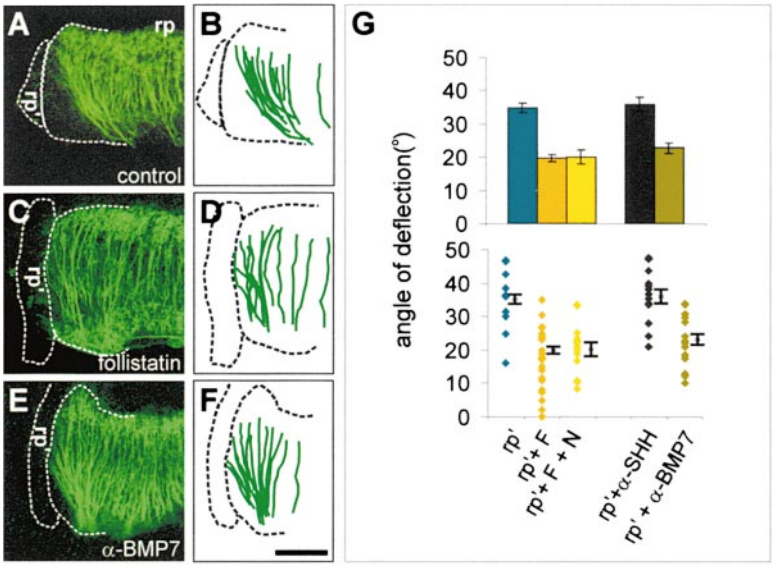

Figure 7. Antagonists of BMPs Reduce the Chemorepellent Activity of the RP

(A–F) d-sc explants grown with appended RP explants (rp′) alone (A and B) or in the presence of follistatin (C and D) or α-BMP7 Ig (E and F). The ability of RP explants to reorient C axons was substantially reduced by follistatin and α-BMP7 Ig. (G) Histograms showing the average (top) and range, mean, and SEM (bottom) of angles of deflection of C axons in d-sc explants grown for 30 hr under control and test conditions. RP explants alone (aquamarine) caused a mean deflection of 34.9° ± 1.4 SEM, n = 72. In the presence of follistatin (rp′ + F, yellow), the average angle of deflection was 19.6° ± 1.1 SEM, n = 87. This represents a significant reduction (assessed by student's t test, $p < 0.006$). In the presence of follistatin and noggin together (rp′ + F + N; paler yellow), the average angle was 20.2° ± 2.2 SEM, n = 16. In the presence of control α-SHH Ig (gray), the angle of deflection was 36.0° ± 2.2 SEM, n = 13, and in α-BMP7 Ig (green), the angle was 22.7° ± 1.7 SEM, n = 17. The inducing activity of mouse RP explants on chick neural plate explants is blocked completely by a combination of follistatin and noggin (Lee et al., 1998). Failure to block completely the axon orienting activity of the RP explant could result from incomplete access of the antagonists in these explant cultures or from the increased sensitivity of the orientation response to BMPs when compared with the induction response (Figure 6). Alternatively, the results may indicate the presence of additional RP BMPs that are refractory to the inhibitory actions of follistatin and noggin or the presence of other chemorepellent factors. Scale bar, 150 μm.

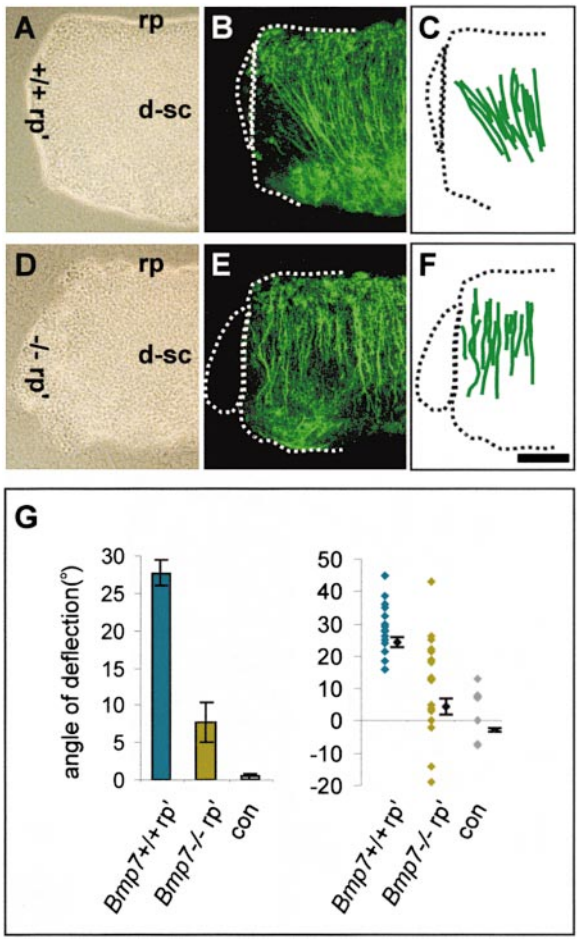

Figure 8. The Ability of the RP to Reorient C Axons Is Reduced in *Bmp7* Mutant Mice

(A–F) d-sc explants cultured for 30 hr with RP explants from wild-type (A–C) and *Bmp7*$^{-/-}$ (D–F) mice. Scale bar, 150 μm.

(G) Average deflection (left) and range, mean, and SEM of angles (right) evoked by RP explants (rp′) from wild-type and mutant mice and the angle of deflection in control (distal end) regions of the d-sc explants. Wild-type RP caused a deflection of 27.7° ± 1.7 SEM (n = 20). Mutant RP explants evoked a deflection of 7.8° ± 3.0 SEM (n = 30). This was significantly different ($p < 9 \times 10^{-7}$) from the D–V trajectory of the axons in control distal regions of the dorsal explants: 6.3° ± 0.3 SEM, n = 40.

explant was reduced to an extent similar to that observed with follistatin alone (Figure 7G). These results support the idea that BMP7, and possibly BMP6, but not noggin-sensitive BMPs, contribute to the repellent activity of the RP.

Anti-BMP7 IgG Blocks RP Activity

To assess further the role of BMP7 as an endogenous mediator of the repellent activity of the RP, we tested the effect of a function-blocking anti-BMP7 Ig (Vukicevic et al., 1994; Dale et al., 1997). In the presence of anti-BMP7 Ig (Figures 8E and 8F), the angle of deflection of C axons evoked by an RP explant was reduced from 35° to 22° (Figures 8E–8G). In the presence of control Ig (anti-SHH Ig; Ericson et al., 1995), the RP explant deflected C axons by an average angle of 35° (Figure 8G). The anti-BMP7 Ig exhibits selectivity for BMP7 over a number of other BMPs, including BMP4 (Vukicevic et al., 1994), but it is unclear whether the activity of BMP6 is also inhibited. Nevertheless, taken together with the orienting potencies of BMP7 and BMP6, these results provide further support for the idea that BMP7 is a component of the endogenous RP repellent signal.

Genetic Evidence for a Role for BMP7 in the Orienting Activity of the RP

To determine whether BMP7 is required for RP activity, RP tissue derived from *Bmp7* mutant mice was tested for repellent activity. RP explants from wild-type mice reoriented C axons in rat d-sc explants by 28° (Figures 8A, 8C, and 8G). In contrast, RP explants from homozygous *Bmp7*$^{-/-}$ mice showed a markedly reduced ability to deflect axons, with an average angle of deflection of only 7° (Figures 8D–8G). This result provides genetic evidence that BMP7 is a required component of the chemorepellent activity of the RP.

BMP7 Can Act Directly on C Growth Cones

We next tested whether BMPs can act directly on the growth cones of C axons. Dissociated dorsal spinal cord cells were grown overnight, to permit neurite extension, exposed to supernatant from *BMP7*- or vector-transfected COS cells for 30 min (Figure 9A), and then fixed. Neurons were labeled with anti-TAG-1 (Figures 9H–9J), to identify C axons, and with anti-erm (Figures 9B–9G) (Birgbauer et al., 1991) or rhodamine phalloidin (data not shown), to reveal growth cone morphology.

In cultures exposed to supernatant from vector-transfected COS cells, C neuron growth cones had an average area of approximately 40 μm^2 and were complex, with approximately five to six major filopodial processes (Figures 9B–9D, 9H, 9I, 9K, and 9L). In contrast, after 30 min exposure to BMP7, the average length of neurites emerging from individual neurons was not altered (Figure 9M), but growth cone area was reduced by 50%–60% (Figures 9E–9G, 9K, 9N, and 9O) and the number of processes by approximately 60% (Figures 9E–9G and 9L). In addition, the distribution of cytoskeletal components recognized by anti-erm Ig changed. In control cultures, growth cones were heavily labeled and axon shafts only lightly labeled by α-erm Ig (Figures 9D–9F). In the presence of BMP7, the proximal-to-distal difference in the labeling along the axon shafts was lost (Figures 9G–9I).

To control for the possibility that BMP7 secreted by COS cells induces the expression of another, non-BMP, factor, we tested the ability of follistatin and anti-BMP7 Ig to block the growth cone collapse evoked by supernatant from BMP7-expressing COS cells. BMP7 supernatant caused a 60% reduction in the area of C growth cones (Figures 9N and 9O), and addition of either follistatin or anti-BMP7 Ig, but not of control Ig, restored growth cone size to 89% of control (Figures 9N and 9O). This result suggests that the collapse of growth cones in these experiments was evoked by BMP7. Thus, BMP7 appears to act directly on C growth cones to elicit a rapid change in cytoskeletal organization and growth cone collapse.

Discussion

We show here that the RP is the source of a diffusible factor that repels C axons and suggest that BMPs mediate the repellent activity of the RP. Several *Bmp*s are

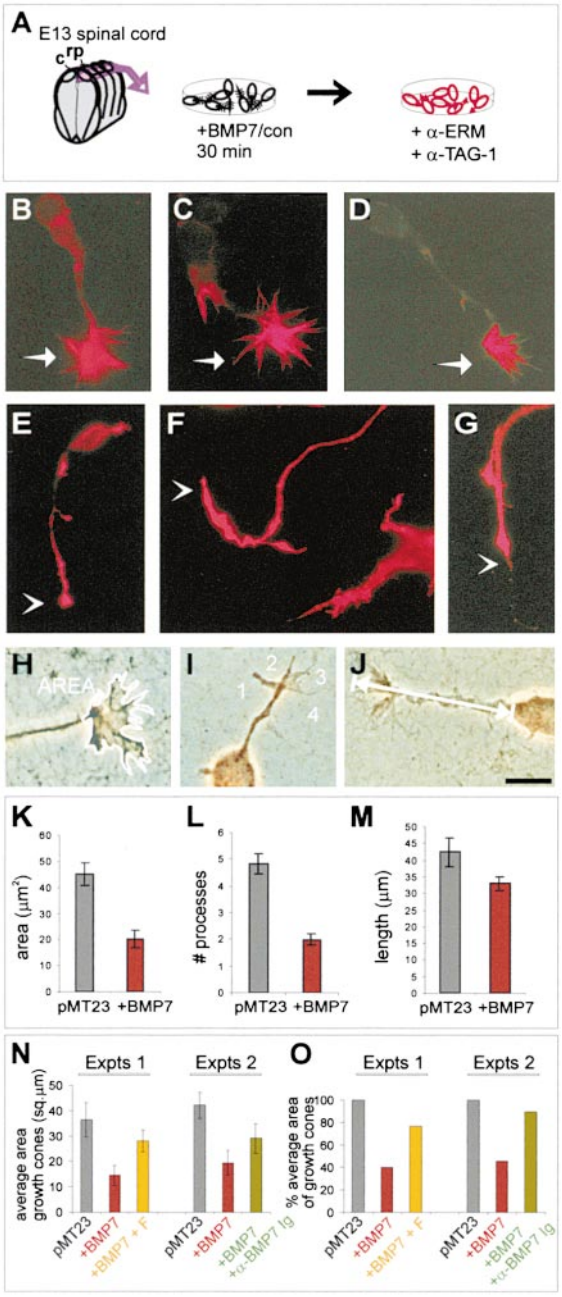

Figure 9. BMP7 Causes Collapse of C Growth Cones

(A–J) Experimental design. (A) A small region (purple) of E13 rat dorsal spinal cord was dissociated and plated onto collagen. Neurites were permitted to extend and then exposed to control or BMP7-expressing COS cell–conditioned medium (CM) for 30 min. (More than 90% of the neurons in these cultures expressed TAG-1.) (B–J) Growth cones were labeled with α-erm (B–G) or α-TAG-1 (H–J) and were photographed and analyzed by estimating area (H), number of major filopodial processes (I), and length of axon (J), using NIH Image.

(B–D) C growth cones exposed to control COS cell–CM.

(E–G) C growth cones exposed to BMP7-expressing COS cell–CM.

(K and M) Effect of BMP7 on growth cone area (K), process number (L), and length (M). The reduction in area from 45.0 ± 4.3 μm^2 SEM (n = 40) to 20.0 ± 3.4 μm^2 SEM (n = 60) is significant ($p < 6.2 \times 10^{-6}$, students t test) as is the reduction in process number from 4.8 ± 0.4 (n = 40) to 2.0 ± 0.2 SEM (n = 60) ($p < 1.0 \times 10^{-9}$). The reduction in length from 42.3 ± 4.3 (n = 40) to 33.0 ± 2.0 (n = 60) was only slight.

(N and O) Average area of C growth cones exposed for 30 min to control COS cell–CM or BMP7-containing supernatant and the effects of follistatin and α-BMP7 Ig on the collapse activity. Results from the two sets of experiments are presented separately, and both are shown as average values (N) and as percentages of control values (O). Expts 1: BMP7-COS cell supernatant caused an average decrease of 60% in growth cone area from 36.5 μm^2 ± 6.8 SEM (n = 6) in control supernatant (gray bars) to 14.5 μm^2 ± 16 (n = 15). Follistatin prevented the BMP7-evoked decrease in area (yellow bars; average area 28.1 μm^2 ± 11, n = 11; represents 77% of control). Expts 2: in a separate series of experiments, BMP7-expressing COS cell supernatant caused a decrease of 54% in growth cone area from 42.2 μm^2 ± 5.1 SEM, n = 13, in control supernatant (gray bars) to 19.5 μm^2 ± 5 SEM, n = 20. In α-BMP7 Ig (green bars), the decrease in area was prevented. Average area was 29.2 μm^2 ± 5.8 SEM, n = 12, representing 70% of control. Scale bar, 10 μm.

present in the rat RP at the time that the axons of dorsal neurons extend, but only BMP7 effectively mimics the repellent effect of the RP on C axons. Antagonists of specific BMPs markedly reduce the repellent signal from the RP. Furthermore, BMP7 can act directly on the growth cones of C axons, causing a rapid change in growth cone morphology. Together, these findings implicate BMPs as axonal repellents, expanding the range of BMP actions in the early patterning of neural cell types and their connections.

RP Repellent Activity Is Diffusible and Appears to Act Directly on a Subset of Axons

The observation that C axons extending into a collagen gel were repelled at a distance by the RP indicates that the RP activity is diffusible. This apparently distinguishes the activity of the RP from a previously described contact inhibitory RP activity thought to create a transient barrier to DRG axons (Snow et al., 1990a, 1990b). The glycosaminoglycan, keratan sulphate, is expressed by the RP coincident with primary sensory axon exclusion from the dorsal midline (Snow et al., 1990b) and inhibits DRG axon extension on laminin when added to the substrate in combination with chondroitin sulphate (Snow et al., 1990a). In contrast to C axons, DRG neurites were not affected by the RP when the explants were placed at a distance from each other.

Orientation of C axon growth does not appear to be secondary to an effect of the RP on the differentiation of cells in the d-sc explant, since ectopic dorsal cell types were not detected. This finding, coupled with the rapid reorientation of growth cones, argues strongly against the idea that a novel cell type is induced in the d-sc explants as a result of exposure to RP signals. The lack of response to the inductive activity of the RP may result from the fact that the d-sc explants used in this assay have lost competence for induction. Consistent with this, mouse spinal cord explants have been shown to have rapidly declining competence for dorsal cell induction (Lee et al., 1998).

BMPs as Axon-Orienting Molecules

The induction of distinct classes of neurons at specific locations within the neural tube is mediated by secreted growth factors provided by restricted groups of cells

(Tanabe and Jessell, 1996). The subsequent guidance of axons toward their targets is mediated by attractant and repellent guidance cues that are generated locally or emanate from distant targets to orient growth cones (Tessier-Lavigne and Goodman, 1996). These two distinct phases of neural development, induction and axon guidance, may in some cases be influenced by a single class of secreted factors. For example, fibroblast growth factors appear to influence the generation of distinct neural cells in the retina and subsequently influence the growth of retinal axons (McFarlane et al., 1996, 1998). Moreover, hepatocyte growth factor, a factor implicated in neural induction (Stern et al., 1990), acts later as a trophic and chemoattractant factor for motor axons (Ebens et al., 1996). The specific roles individual factors play in the patterning of the CNS thus appear to depend on the state of differentiation of responsive cells.

BMPs have previously been implicated in the survival, induction, and differentiation of a wide range of neural cells (Perides et al., 1993; Liem et al., 1995; Gross et al., 1996; Hogan, 1996; Shah et al., 1996; Guo et al., 1998). Our results provide evidence for an additional role for BMPs in repelling the growth cones of developing axons and thus patterning axonal projections. Several TGFβ family members, including BMP7, have been shown to elicit chemotaxis by peripheral blood monocytes and polymorphonuclear leukocytes (Cunningham et al., 1992; Postlethwaite et al., 1994). In addition, a TGFβ family member, unc-129, has been implicated in the guidance of motor axons in *C. elegans* (Colavita et al., 1998). Whether unc-129 acts directly on the growth cones, however, remains unclear. Together, these findings raise the possibility that BMPs regulate both the directed migration of cells and the extension of axons.

A Contribution of BMP7 to the Repellent Activity of the RP

Our results indicate that BMP7 is the major component of the RP-derived chemorepellent activity for C axon guidance. BMP6 reorienting activity appears to represent only a minor component of the RP signal. However, the potential for BMP6 to form heterodimers with other BMPs (Israel et al., 1996) leaves open the possibility that BMP6 could have a larger contribution to the activity of the RP in vivo than predicted on the basis of our experiments. Assays of the activity of the RP from *Bmp6* mutant mice should clarify this issue.

The residual repellent activity in the RP from the *Bmp7* mutant mouse may reflect the activity of another unidentified BMP or signaling molecule unrelated to the BMP family. Several other potential guidance factors expressed by the RP fail to repel C axons (Table 1; Brose et al., 1999). However, these results do not yet exclude the possibility that molecules other than BMPs also contribute to RP repellent activity.

The Specificity of BMP Action Suggests Novel Structure–Activity Relationships within the BMP Family

One striking feature of our findings is that the ability of individual BMPs to reorient C axons does not parallel their ability to induce the differentiation of dorsal spinal cord cell types. All BMPs and many other members of the TGFβ superfamily induce dorsal neurons (Liem et al., 1997; Lee et al., 1998). In contrast, BMP7, BMP6, and BMP4, but neither other BMPs (Dsl1 and GDF7) nor TGFβs (ActβB and cVg1), exhibit C axon orienting activity. Moreover, the relative potencies of BMPs with repellent activity do not conform with conventional structural groupings. BMP6 and BMP7 are highly related (Celeste et al., 1990; Hahn et al., 1992; Gitelman et al., 1997) and in inductive assays have essentially indistinguishable activities (Liem et al., 1997; Lee et al., 1998). However, BMP6 is only weakly active in C axon reorientation compared to BMP7, even though it was as effective as BMP7 in inducing the ectopic expression of dorsal markers in the d-sc explants, apparently a less sensitive assay than axon reorientation. These results suggest that the low-level orienting activity of BMP6 is not due to limited availability of BMP6 to neural cells but reflects, instead, a difference in the C axon response to BMP7 and BMP6. Further evidence for a novel profile of responses to BMPs comes from the results of testing BMP4 in our assay. BMP4 is a member of a distinct structural subgroup, the BMP2/4 class, yet appeared as potent as BMP7 in orientation of C axons. Taken together, our results suggest an unorthodox structure–activity relationship of BMPs in reorienting growth cones.

Growth Cones Respond to BMP7 Directly

The ability of a factor to evoke the morphological changes associated with growth cone collapse appears to correlate with axon-reorienting ability (Fan and Raper, 1995). The direct and rapid action of BMP7 on growth cones in vitro supports the possibility that it acts as a repellent to guide C axons.

BMPs typically interact with heterodimeric serine/threonine kinase receptors whose activation leads to phosphorylation and nuclear translocation of SMAD proteins that then regulate the transcription of target genes (Hogan, 1994; ten Dijke et al., 1994; Whitman, 1997; Kretzschmar and Massague, 1998). However, the time course of C growth cone collapse and the localization of the response to the growth cone itself are difficult to reconcile with the idea that a transcriptional cascade mediates the orienting effects of BMP7. The timing and nature of the chemotactic response of peripheral blood monocytes to BMP7 (Cunningham et al., 1992) also suggest a nontranscriptional response. These orientating responses could involve a second messenger cascade independent of SMADs or may involve nontransciptional pathways downstream of SMADs.

Some of the cytoplasmic components that have been implicated in growth cone extension have been reported to be activated in the response to TGFβs. BMPs have been shown to activate PKA (Lee and Chuong, 1997) and other TGFβ family members appear to stimulate phospholipase C, PKC, and rho GTPase (Halstead et al., 1995; Choi et al., 1999). Many second messenger systems that mediate growth cone turning responses to chemotropic signals and direct the rearrangement of the cytoskeleton necessary for navigation have been identified (Mueller, 1999). Further studies may resolve whether the mechanisms by which BMPs orient growth cones of C axons involve the activation of one or several of these pathways.

Roles of BMP7 in the Guidance of Dorsal Spinal Cord Axons

Our experiments have not addressed the cellular mechanisms by which BMPs influence the trajectory of C axons in vivo. A factor that can reorient growth cones may also act in vivo to establish internal polarity in dorsal neurons before overt axon extension, since the underlying cytoskeletal events may be similar (Spiegelman et al., 1979; Tanaka and Sabry, 1995). Furthermore, the distribution of *BMP7* in the rat spinal cord, both in and around the RP, provides sources of polarizing information that may shape the C axon projections both early and late in axon extension through the dorsal spinal cord. Preliminary analysis of the *Bmp7* mutant mouse spinal cord suggests that there is a defect in C axon extension in the early spinal cord (our unpublished data).

It remains unclear how many classes of dorsal spinal axons are influenced by the RP-derived repellent. This study does not address the precise range over which the RP signal or individual BMPs act within dorsal neuroepithelium, but our in vitro results indicate that axons reorient within approximately 150 μm, a range in principle sufficient to influence many classes of dorsal interneurons at the time that they first extend axons. Within the dorsal spinal cord, several classes of interneuron reside in positions within the potential range of the RP (Nornes and Das, 1974; Altman and Bayer, 1984; Liem et al., 1997; Lee et al., 1998). Interneurons that develop at early stages within the dorsal half of the spinal cord include both the C neurons and a class of ipsilaterally projecting association neurons (Holley, 1982; Holley et al., 1982; Dodd et al., 1988). Both classes of neurons initially project their axons ventrally and circumferentially, raising the possibility that the axons of classes of other spinal interneurons respond to RP repellent activity.

Complementary Roles of the RP and the FP

The RP appears to play a pivotal role in the early development of the dorsal spinal cord, inducing dorsal spinal interneurons and patterning their initial projections. The identification of an RP-derived diffusible guidance cue that can orient C axons within the dorsal half of the spinal cord supports a model in which both the RP and the FP contribute inductive and guidance cues to adjacent neurons. The RP chemorepellent activity potentially acts in the early stages of C axon extension whereas netrin-1 guides C axons through a later phase, suggesting that the RP and the FP are complementary midline organizing centers that act in a sequential manner to guide sets of C axons within the developing CNS.

The inductive and axon patterning functions of the FP, however, appear to be mediated by distinct signals. The secretion of SHH by the FP is essential for the differentiation of motor neurons and ventral interneurons (Roelink et al., 1994; Marti et al., 1995; Chiang et al., 1996; Ericson et al., 1996, 1997), whereas netrin-1 and other FP-associated factors appear to regulate the axon projections of dorsal spinal interneurons and motor neurons (Tessier-Lavigne et al., 1988; Placzek et al., 1990; Bovolenta and Dodd, 1991; Kennedy et al., 1994; Serafini et al., 1994, 1996; Colamarino and Tessier-Lavigne, 1995; Guthrie and Pini, 1995; Stoeckli and Landmesser, 1995). In the dorsal spinal cord, the RP may achieve these two roles in the development of dorsal C neurons through the distinct and sequential activities of a single class of signaling molecules, the BMPs.

Experimental Procedures

Explant Cultures

d-sc and RP explants were dissected at a level caudal to the forelimb of E11 or E13 embryos (Tessier-Lavigne et al., 1988) and embedded in collagen gels (Lumsden and Davies, 1986). Explants were cultured for 15–35 hr in Opti-MEMI (GIBCO-BRL) (with pen/strep/L-glu; Sigma). Netrin-1 (Serafini et al., 1994) was also included in the medium of E13 d-sc explants.

DiI Labeling

Following fixation in 4% paraformaldehyde, the top layer of collagen was removed and crystals of DiI placed in the d-sc explants. Cultures were incubated at 4°C, for1–4d, in PBS. Photographic slides of E13 d-sc explants, DiI labeled, were projected onto a screen and neurites measured as in Figure 2M.

Antibodies

Antibodies used were α-TAG-1 (mAb 4D7; Dodd et al., 1988), rabbit α-pLH2 (Liem at al., 1997), rabbit α-Isl1/2 (Liem et al., 1997), rabbit α-MafB (Eichmann et al., 1997), and rabbit α Math1 (Helms and Johnson, 1998) and α-erm (mAb 13H9; Goslin et al., 1989). Cultured neurons were labeled with 4D7 or 13H9 or with rhodamine-phalloidin to detect F-actin.

Whole-Mount In Situ Hybridization

Mouse *Bmp6*, *Bmp7*, and *Gdf7* riboprobes were used on E12 or E13 rat spinal cord cryostat sections (Schaeren-Wiemers and Gerfin-Moser, 1993).

COS Cell Transfections

COS-7 cells were transfected using Lipofectamine (GIBCO-BRL) and aggregated (Shah et al., 1997). *BMP7*, *BMP4*, *Vg1*, *Collapsin2*, *Dsl*, *ActβB* (chick homologs), *Gdf7*, and *Bmp6* (mouse homologs) were expressed using pMT23 (Hume and Dodd, 1993). *Wnt1* (mouse), *Wnt3* (human/murine hybrid), *Wnt3a*, and *Wnt4* (mouse) were expressed with pLNCx, pGEM, or pGEM72 (gifts of Jan Kitajewski). All *BMP* constructs consisted of the mature region of the individual BMP and the proregion of BMP2 (Liem et al., 1997; Shah et al., 1997; Lee et al., 1998). Aggregates of transfected cells, comparable in size to an RP explant, were appended to d-sc explants. To vary the dose of BMPs, aggregates were made by mixing appropriate numbers of COS cells from plates in which cells were transfected with a *BMP* in ratios with cells expressing pMT23 alone. COS cells were not selected for BMP expression; thus, mixed cell clumps included nontransfected COS cells. The percent values represent dilution rather than actual numbers of transfected COS cells.

COS Cell–Conditioned Medium

The medium was replaced with serum-free Opti-MEMI (+pen/strep/L-glu) 12–18 hr after transfection of COS cells with pMT23 or *Bmp7*, and COS cell–conditioned medium (CM) was collected 48–72 hr later.

Dissociated Cell Culture

Neural tissue obtained from a small region adjacent to the E13 rat RP was dissociated and plated on collagen substrate at low density to permit visualization of individual growth cones. The dorsal fifth of E13 spinal cord was dissociated using trypsin (0.05% GIBCO-BRL) for 10 min at 37°C followed by trituration. Cells were plated on collagen and incubated for 18–24 hr in Opti-MEM 10% FBS at 37°C in 5% CO_2. Medium was changed to serum-free Opti-MEM containing BMP7- or pMT23-CM for 30 min and fixed in prewarmed (37°C) 4% paraformaldehyde ± 0.5% glutaraldehyde for 5 min.

Analysis of Growth Cone Morphology

Neurons in randomly chosen areas of each culture with processes greater than 10 μm were photographed, and the images were

scanned. The area, length, and number of major processes of each growth cone was measured using NIH Image.

Analysis of BMP Antagonists

Follistatin (National Hormone and Pituitary Program) (2 μg/ml), noggin (gift of R. Harland) (500 ng/ml), α-BMP7 Ig, 1B12 (gift of K. Sampath, Creative Biomolecules) (10 μg/ml), and α-SHH Ig, 5E1 (gift of T. Jessell) (10 μg/ml), were included in the culture medium.

Analysis of *Bmp7* Mutant Mice

Homozygous *Bmp7* mutant embryos (gift of E. Robertson) were genotyped by PCR (Dudley et al., 1995). *Bmp7*$^{-/-}$ embryos E10.5 and older could also be identified by a defect in eye development (Dudley et al., 1995).

Acknowledgments

We are grateful to R. Harland for noggin, K. Lee for chordin, J. Raper for collapsin cDNAs, M. Tessier-Lavigne for the netrin expression vector, J. Kitajewski for wnts, and E. Robertson for *Bmp7* mutant mice. Antibodies were provided by J. Johnson (α-mATH-1), T. Jessell (α-LH2A/B, α-Isl 1, and α-SHH), M. Nishizawa (α-MafB), K. Sampath (α-BMP7), and F. Solomon (α-ezrin). We are indebted to J. Briscoe and S. Sockanathan for advice on confocal microscopy. We wish to thank L. Greene, T. Jessell, M. Placzek, and members of the Dodd and Jessell labs for helpful discussions and to J. Heemskerk, T. Jessell, K. Lee, and C. Mason for comments on the manuscript. The work was funded by a grant from the NIH, NS 27113, to J. D.

Received May 24, 1999; revised August 10, 1999.

References

Altman, J., and Bayer, S.A. (1984). The development of the rat spinal cord. Adv. Anat. Embryol. Cell Biol. *85*, 1–164.

Basler, K., Edlund, T., Jessell, T.M., and Yamada, T. (1993). Control of cell pattern in the neural tube: regulation of cell differentiation by dorsalin-1, a novel TGFB family member. Cell *73*, 687–702.

Bergemann, A.D., Zhang, L., Chiang, M., Brambilla, R., Klein, R., and Flanagan, J.G. (1998). Ephrin-B3, a ligand for the receptor EphB3, expressed at the midline of the developing neural tube. Oncogene *16*, 471–480.

Birgbauer, E., Dinsmore, J.H., Winckler, B., Lander, A.D., and Solomon, F. (1991). Association of ezrin isoforms with the neuronal cytoskeleton. J. Neurosci. Res. *30*, 232–241.

Bovolenta, P., and Dodd, J. (1990). Guidance of commissural growth cones at the floor plate in embryonic rat spinal cord. Development *109*, 435–477.

Bovolenta, P., and Dodd, J. (1991). Perturbation of neuronal differentiation and axon guidance in the spinal cord of mouse embryos lacking a floor plate: analysis of Danforth's short-tail mutation. Development *113*, 625–639.

Brose, K., Bland, K.S., Wang, K.H., Arnott, D., Henzel, W., Goodman, C.S., Tessier-Lavigne, M., and Kidd, T. (1999). Slit proteins bind robo receptors and have an evolutionarily conserved role in repulsive axon guidance. Cell *96*, 795–806.

Celeste, A.J., Iannazzi, J.A., Taylor, R.C., Hewick, R.M., Rosen, V., Wang, E.A., and Wozney, J.M. (1990). Identification of transforming growth factor-β family members present in bone-inductive protein purified from bovine bone. Proc. Natl. Acad. Sci. USA *87*, 9843–9847.

Chiang, C., Litingtung, Y., Lee, E., Young, K.E., Corden, J.L., Westphal, H., and Beachy, P.A. (1996). Cyclopia and defective axial patterning in mice lacking Sonic hedgehog gene function. Nature *383*, 407–413.

Choi, S.E., Choi, E.Y., Kim, P.H., and Kim, J.H. (1999). Involvement of protein kinase C and rho GTPase in the nuclear signaling pathway by transforming growth factor-beta1 in rat-2 fibroblast cells. Cell Signal *11*, 71–76.

Colamarino, S., and Tessier-Lavigne, M. (1995). The axonal chemoattractant netrin-1 is also a chemorepellent for trochlear motor axons. Cell *81*, 621–629.

Colavita, A., Krishna, S., Zheng, H., Padgett R.W., and Culotti, J.G. (1998). Pioneer axon guidance by UNC-129, a C. elegans TGF-beta. Science *281*, 706–709.

Cunningham, N.S., Paralkar, V., and Reddi, A.H. (1992). Osteogenin and recombinant bone morphogenetic protein 2B are chemotactic for human monocytes and stimulate transforming growth factor beta 1 mRNA expression. Proc. Natl. Acad. Sci. USA *89*, 11740–11744.

Dale, K., Vesque, C., Sattar, N., Lints, T., Sampath, K., Furley, A., Dodd, J., and Placek, M. (1997). Cooperation of BMP7 and SHH in the induction of forebrain ventral midline cells by prechordal mesoderm. Cell *90*, 257–269.

Dodd, J., Morton, S.B., Karagogeos, D., Yamamoto, M., and Jessell, T.M. (1988). Spatial regulation of axonal glycoprotein expression on subsets of embryonic spinal neurons. Neuron *1*, 105–116.

Dudley, A.T., Lyons, K.M., and Robertson, E.J. (1995). A requirement for bone morpohogenetic protein-7 during development of the mammalian kidney and eye. Genes Dev. *9*, 2795–2807.

Dudley, A.T., and Robertson, E.J. (1997). Overlapping expression domains of bone morphogenetic protein family members potentially account for limited tissue defects in BMP7 deficient embryos. Dev. Dyn. *208*, 349–362.

Ebens, A., Brose, K., Leonardo, E.D., Hanson, M.G. Jr., Bladt, F., Birchmeier, C., Barres, B.A., and Tessier-Lavigne, M. (1996). Hepatocyte growth factor/scatter factor is an axonal chemoattractant and a neurotrophic factor for spinal motor neurons. Neuron *17*, 1157–1172.

Eichmann, A., Grapin-Botton, A., Kelly, L., Graf, T., Le Douarin, N.M., and Sieweke, M. (1997). The expression pattern of the mafB/kr gene in birds and mice reveals that the kreisler phenotype does not represent a null mutant. Mech. Dev. *65*, 111–122.

Ericson, J., Muhr, J., Placzek, M., Lints, T., Jessell, T.M., and Edlund, T. (1995). Sonic hedgehog induces the differentiation of ventral forebrain neurons: a common signal for ventral patterning within the neural tube. Cell *81*, 747–756.

Ericson, J., Morton, S., Kawakami, A., Roelink, H., and Jessell, T.M. (1996). Two critical periods of Sonic hedgehog signaling required for the specification of motor neuron identity. Cell *87*, 661–673.

Ericson, J., Rashbass, P., Schedl, A., Brenner-Morton, S., Kawakami, A., van Heyningen, V., Jessell, T.M., and Briscoe, J. (1997). Pax6 controls progenitor cell identity and neuronal fate in response to graded Shh signaling. Cell *90*, 169–180.

Evan, G.I., Lewis, G.K, Ramsay, G., and Bishop, J.M. (1985). Isolation of monoclonal antibodies specific for human c-myc protooncogene product. Mol. Cell. Biol. *5*, 3610–3616.

Fan, J., and Raper, J.A. (1995). Localized collapsing cues steer growth cones without inducing their full collapse. Neuron *14*, 263–274.

Fazeli, A., Dickinson, S.L., Hermiston, M.L., Tighe, R.V., Steen, R.G., Small, C.G., Stoeckli, E.T., Keino-Masu, K., Masu, M., Rayburn, H., et al. (1997). Phenotype of mice lacking functional Deleted in colorectal cancer (Dcc) gene. Nature *386*, 796–804.

Furuta, Y., Piston, D.W., and Hogan, B.L. (1997). Bone morphogenetic proteins (BMPs) as regulators of dorsal forebrain development. Development *124*, 2203–2212.

Gale, N.W., Flenniken, A., Compton, D.C., Jenkins, N., Copeland, N.G., Gilbert, D.J., Davis, S., Wilkinson, D.G., and Yancopoulos, G.D. (1996). Elk-L3, a novel transmembrane ligand for the Eph family of receptor tyrosine kinases,expressed in embryonic floor plate, roof plate and hindbrain segments. Oncogene *19*, 1343–1352.

Gitelman, S.E., Kobrin, M., Lee, A., Fet, V., Lyons, K., Hogan, B.L.M., and Derynck, R. (1997). Structure and sequence of the mouse *Bmp6* gene. Mamm. Genome *8*, 212–214.

Goslin, K., Birgbauer, E., Banker, G., and Solomon, F. (1989). The role of cytoskeleton in organizing growth cones: a microfilament-associated growth cone component depends upon microtubules for its localization. J. Cell Biol. *109*, 1621–1631.

Graham, A., Francis-West, P., Brickell, P., Lumsden, A. (1994). The signaling molecule BMP4 mediates apoptosis in the rhombencephalic neural crest. Nature *372*, 684–686.

Gross, R.E., Mehler, M.F., Mabie, P.C., Zang, Z., Santschi, L., and Kessler, J.A. (1996). Bone morphogenetic proteins promote astroglial lineage commitment by mammalian subventricular zone progenitor cells. Neuron *17*, 595–606.

Guo, X., Rueger, D., and Higgins, D. (1998). Osteogenic protein-1 and bone morphogenetic proteins regulate dendritic growth and the expression of microtubule-associated protein-2 in rat sympathetic neurons. Neurosci. Lett. *245*, 131–134.

Guthrie, S., and Pini, A. (1995). Chemorepulsion of developing motor axons by the floor plate. Neuron *14*, 1117–1130.

Hahn, G.V., Cohen, R.B., Wozney, J.M., Levitz, C.L., Shore, E.M., Zasloff, M.A., and Kaplan, F.S. (1992). A bone morphogenetic protein subfamily: chromosomal localization of human genes for BMP5, BMP6, and BMP7. Genomics *14*, 759–762.

Halstead, J., Kemp, K., and Ignotz, R.A. (1995). Evidence for involvement of phosphatidylcholine-phospholipase C and protein kinase C in transforming growth factor-beta signaling. J. Biol. Chem. *270*, 13600–13603.

Helms, A.W., and Johnson, J.E. (1998). Progenitors of C interneurons are defined by MATH1 expression. Development *125*, 919–928.

Hogan, B.L. (1994). Sorting out the signals. Curr. Biol. *4*, 1122–1124.

Hogan, B.L. (1996). Bone morphogenetic proteins in development. Curr. Opin. Genet. Dev. *6*, 432–438.

Holley, J.A. (1982). Early development of the circumferential axonal pathway in mouse and chick spinal cord. J. Comp. Neurol. *205*, 371–382.

Holley, J.A., Nornes, H.O., and Morita, M. (1982). Guidance of neuritic growth in the transverse plane of embryonic mouse spinal cord. J. Comp. Neurol. *205*, 360–370.

Hume, C.R., and Dodd, J. (1993). Cwnt-8C: a novel Wnt gene with a potential role in primitive streak formation and hindbrain organization. Development *119*, 1147–1160.

Israel, D.I., Nove, J., Kerns, K.M., Kaufman, R.J., Rosen, V., Cox, K.A., and Wozney, J.M. (1996). Heterodimeric bone morphogenetic proteins show enhanced activity in vitro and in vivo. Growth Factors *13*, 291–300.

Jones, C.M., Lyons, K.M., and Hogan, B.L. (1991). Involvement of bone morphogenetic protein-4 (BMP-4) and Vgr-1 in morphogenesis and neurogenesis in the mouse. Development *111*, 531–542.

Kennedy, T.E., Serafini, T., de la Torre, J., and Tessier-Lavigne, M. (1994). Netrins are chemotropic factors for C axons in the embryonic spinal cord. Cell *78*, 425–435.

Kretzschmar, M., and Massague, J. (1998). SMADs: mediators and regulators of TGFβ signaling. Curr. Opin. Genet. Dev. *8*, 103–111.

Lee, Y.S., and Chuong, C.M. (1997). Activation of protein kinase A is a pivotal step involved in both BMP-2- and cyclic AMP-induced chondrogenesis. J. Cell Physiol. *170*, 153–165.

Lee, K.J., and Jessell, T.M. (1999). The specification of dorsal cell fates in the vertebrate central nervous system. Annu. Rev. Neurosci. *22*, 261–294.

Lee, K.J., Mendelsohn, M., and Jessell, T.M. (1998). Neuronal patterning by BMPs: a requirement for GDF7 in the generation of a discrete class of commissural interneurons in the mouse spinal cord. Genes Dev. *12*, 3394–3407.

Li, H., Chen, J., Wu, W., Fagaly, T., Zhou, L., Yuan, W., Dupuis, S., Jiang, Z., Nash, W., Gick, C., et al. (1999). Vertebrate slit, a secreted ligand for the transmembrane protein roundabout, is a repellent for olfactory bulb axons. Cell *96*, 807–818.

Liem, K.F., Jr., Tremml, G., Roelink, H., and Jessel, T.M. (1995). Dorsal differentiation of neural plate cells induced by BMP-mediated signals from epidermal ectoderms. Cell *82*, 969–979.

Liem, K.F., Jr., Tremml, G., and Jessell, T.M. (1997). A role for the roof plate and its resident TGFβ-related proteins in neuronal patterning in the dorsal spinal cord. Cell *91*, 127–138.

Loschinger, J., Bandtlow, C.E., Jung, J., Klostermann, S., Schwab, M.E., Bonhoeffer, F., and Kater, S.B. (1997). Retinal axon growth cone responses to different environmental cues are mediated by different second messenger systems. J. Neurobiol. *33*, 825–834.

Lumsden, A., and Davies, A. (1986). Chemotropic effect of specific target epithelium in development of the mammalian nervous system. Nature *323*, 538–539.

Luo, Y., Raible, D., and Raper, J.A. (1993). Collapsin: a protein in the brain that induces the collapse and paralysis of neuronal growth cones. Cell *75*, 217–227.

Luo, Y., Shepherd, I., Li, J., Renzi, M.J., Chang, S., and Raper, J.A. (1995). A family of molecules related to collapsin in the embryonic chick nervous system. Neuron *14*, 1131–1140.

Lyons, K.M., Hogan, B.L.M., and Robertson, E.J. (1995). Colocalization of BMP7 and BMP2 RNAs suggests that these factors cooperatively mediate tissue interactions during murine development. Mech. Dev. *50*, 71–83.

Marti, E., Takada, R., Bumcrot, D.A., Sasaki, H., and McMahon, A.P. (1995). Distribution of Sonic hedgehog peptides in the developing chick and mouse embryo. Development *121*, 2537–2547.

McFarlane, S., Cornel, E., Amaya, E., and Holt, C.E. (1996). Inhibition of FGF receptor activity in retinal ganglion cell axons causes errors in target recognition. Neuron *17*, 245–254.

McFarlane, S., Zuber, M.E., and Holt, C.E. (1998). A role for the fibroblast growth factor receptor in cell fate decisions in the developing vertebrate retina. Development *125*, 3967–3975.

Mueller, B.K. (1999). Growth cone guidance: first steps towards a deeper understanding. Annu. Rev. Neurosci. *22*, 351–388.

Nornes, H.O., and Das, G.D. (1974). Temporal pattern of neurogenesis in the spinal cord of rat. I. Time and sites of origin and migration and settling patterns of neuroblasts. Brain Res. *73*, 121–138.

Oppenheim, R.W., Schneiderman, A., Shimizu, I., and Yaginuma, H. (1988). Onset and development of intersegmental projections in the chick embryo spinal cord. J. Comp. Neurol. *275*, 159–180.

Parr, B.A., Shea, M.J., Vassileva, G., and McMahon, A.P. (1993). Mouse Wnt genes exhibit discrete domains of expression in the early CNS and limb buds. Development *119*, 247–261.

Perides, G., Hu, G., Rueger, D.C., and Charness, M.E. (1993). Osteogenic protein-1 regulates L1 and neural cell adhesion molecule gene expression in neural cells. J. Biol. Chem. *268*, 25179–25205.

Placzek, M., Tessier-Lavigne, M., Jessell, T.M., and Dodd, J. (1990). Orientation of commissural axons in vitro in response to a floor plate-derived chemoattractant. Development *110*, 19–30.

Placzek, M., Yamada, T., Tessier-Lavigne, M., Jessell, T.M., and Dodd, J. (1991). Control of dorsoventral pattern in vertebrate neural development: induction and polarizing properties of the floor plate. Dev. Suppl. *2*, 105–122.

Postlethwaite, A., Raghow, R., Stricklin, G., Ballow, L., and Sampath, T. (1994). Osteogenic protein-1 a bone morphogenetic protein member of the TGFβ superfamily shares chemotactic properties but not fibrogenic properties with TGFβ. J. Cell Phys. *161*, 562–570.

Ramon y Cajal, S. (1909). Histologie du Systeme Nerveux de l'Homme et des Vertebres. (Madrid: Consejo Superior de Investigaciones Cientificas).

Roelink, H., and Nusse, R. (1991). Expression of two members of the wnt family during mouse development—restricted temporal and spatial patterns in the developing neural tube. Genes Dev. *5*, 381–388.

Roelink, H., Augsburger, A., Heemskerk, J., Korzh, V., Norlin, S., Ruiz, I., Altaba, A., Tanabe, Y., Placzek, M., Edlund, T., Jessell, T.M., and Dodd, J. (1994). Floor plate and motor neuron induction by vhh-1, a vertebrate homolog of hedgehog expressed by the notochord. Cell *76*, 761–775.

Schaeren-Wiemers, N., and Gerfin-Moser, A. (1993). A single protocol to detect transcripts of various types and expression levels in neural tissue and cultured cells: in situ hybridization using digoxigenin-labelled cRNA probes. Histochemistry *100*, 431–440.

Serafini, T., Kennedy, T.E., Galko, M.J., Mirzyan, C.M., Jessell, T.M., and Tessier-Lavigne, M. (1994). The netrins define a family of axon outgrowth-promoting proteins homologous to C. elegans UNC-6. Cell *78*, 409–424.

Serafini, T., Colamarino, S.A., Leonardo, E.D., Wang, H., Beddington, R., Skarnes, W.C., and Tessier-Lavigne, M. (1996). Netrin-1 is required for commissural axon guidance in the developing vertebrate nervous system. Cell *87*, 1001–1014.

Shah, N.M., Groves, A.K., and Anderson, D.J. (1996). BMP2 and BMP4, but not BMP6, increase the number of adrenergic cells which develop in quail trunk neural crest cultures. Exp. Neurol. *140*, 331–343.

Shah, S., Skromne, I., Hume, C., Kessler, D., Lee, K.J., Stern, C., and Dodd, J. (1997). Misexpression of chick Vg1 in the marginal zone induces primitive streak formation. Development *124*, 5127–5138.

Silos-Santiago, I., and Snider, W.D. (1992). Development of commissural neurons in the embryonic rat spinal cord. J. Comp. Neurol. *325*, 514–526.

Snow, D.M., Lemmon, V., Carrino, D.A., Caplan, A.I., and Silver, J. (1990a). Sulphated proteoglycans in astroglial barriers inhibit neurite outgrowth *in vitro*. Exp. Neurol. *109*, 111–130.

Snow, D.M., Steindler, D.A., and Silver, J. (1990b). Molecular and cellular characterization of the glial roof plate of the spinal cord and optic tectum: a possible role for a proteoglycan in the development of an axon barrier. Dev. Biol. *138*, 359–376.

Spiegelman, B., Lopata, M.A., and Kirschner, M.W. (1979). Aggregation of micrtuble initiation sites preceding neurite outgrowth in mouse neuroblastoma cells. Cell *16*, 253–263.

Stern, C.D., Ireland, G.W., Herrick, S.E., Gherardi, E., Gray, J., Perryman, M., and Stoker, M. (1990). Epithelial scatter factor and development of the chick embryonic axis. Development *110*, 1271–1284.

Stoeckli, E.T., and Landmesser, L.T. (1995). Axonin-1, Nr-CAM, and Ng-CAM play different roles in the in vivo guidance of chick commissural neurons. Neuron *14*, 1165–1179.

Tanabe, Y., and Jessell, T.M. (1996). Diversity and pattern in the developing spinal cord. Science *274*, 1115–1123.

Tanaka, E., and Sabry, J. (1995). Making the connection: cytoskeletal rearrangements during growth cone guidance. Cell *83*, 171–176.

ten Dijke, P., Yamashita, H., Sampath, T.K., Reddi, A.H., Estevez, M., Riddle, D.L., Ichijo, H., Heldin, C.H., and Miyazono, K. (1994). Identification of type I receptors for osteogenic protein I and bone morphogenetic protein-4. J. Biol. Chem. *269*, 16985–16988.

Tessier-Lavigne, M., and Goodman, C.S. (1996). The molecular biology of axon guidance. Science *274*, 1123–1133.

Tessier-Lavigne, M., Placzek, M., Lumsden, A., Dodd, J., and Jessell, T.M. (1988). Chemotropic guidance of developing axons in the mammalian central nervous system. Nature *336*, 775–778.

Vukicevic, S., Latin, V., Chen, P., Batorsky, R., Reddi, A.H., and Sampath, T.K. (1994). Localization of osteogenic protein-1 (bone morphogenetic protein-7) during human embryonic development: high affinity binding to basement membranes. Biochem. Biophys. Res. Commun. *198*, 693–700.

Wang, H.U., and Anderson, D.J. (1997). Eph family transmembrane ligands can mediate repulsive guidance of trunk neural crest migration and motor axon outgrowth. Neuron *18*, 383–396.

Wentworth, L.E. (1984). The development of the cervical spinal cord of the mouse embryo. II. A Golgi analysis of sensory, commissural and association cell differentiation. J. Comp. Neurol. *222*, 96–115.

Whitman, M. (1997). Signal transduction. Feedback from inhibitory SMADs. Nature *389*, 549–551.

Yaginuma, H., Homma, S., Kunzi, R., and Oppenheim, R.W. (1991). Pathfinding by growth cones of C interneurons in the chick embryo spinal cord: a light and electron microscopic study. J. Comp. Neurol. *304*, 78–102.

Yamashita, H., ten Dijke, P., Huylebroeck, D., Sampath, T.K., Andries, M., Smith, J.C., Heldin, C.H., and Miyazono, K. (1995). Osteogenic protein-1 binds to activin type II receptors and induces certain activin-like effects. J. Cell Biol. *130*, 217–226.

Zimmerman, L.B., De Jesus-Escobar, J.M., and Harland, R.M. (1996). The Spemann organizer signal noggin binds and inactivates bone morphogenetic protein 4. Cell *86*, 599–606.